

Electronic Supplementary Information (ESI) for

**A Small Molecule/Fullerene Binary Acceptor System for High-Performance  
Polymer Solar Cells with Enhanced Light-Harvesting Property and  
Balanced Carrier Mobility**

Yang Wang,<sup>a‡</sup> Wei-Dong Xu,<sup>ab‡</sup> Jian-Dong Zhang,<sup>a</sup> Lu Zhou,<sup>a</sup> Gang Lei,<sup>a</sup> Cheng-Fang Liu,<sup>a</sup>  
Wen-Yong Lai<sup>\*ab</sup> and Wei Huang<sup>ab</sup>

<sup>a</sup> Key Laboratory for Organic Electronics and Information Displays & Institute of Advanced Materials (IAM), Jiangsu National Synergetic Innovation Center for Advanced Materials (SICAM), Nanjing University of Posts & Telecommunications, 9 Wenyuan Road, Nanjing 210023, China, E-mail: iamwylai@njupt.edu.cn

<sup>b</sup> Key Laboratory of Flexible Electronics (KLOFE) & Institute of Advanced Materials (IAM), Jiangsu National Synergetic Innovation Center for Advanced Materials (SICAM), Nanjing Tech University (NanjingTech), 30 South Puzhu Road, Nanjing 211816, China

‡ Y. W. and W. X. are co-first authors with equal contribution to this work.

## General Details.

**Device Fabrication and Characterization.** The glass/ITO substrates were pre-cleaned with a special detergent (Alconox Inc.), acetone, isopropanol, and dried under a flow of dry nitrogen. Before deposition of the electron-collecting interlayer, ITO substrates were cleaned in UV azone for 5 min. Inverted devices were fabricated with the structure of ITO/ZnO/active layer/MoO<sub>3</sub>/Ag. The sol-gel derived ZnO films were prepared according to the literature.<sup>[1]</sup> The prepared precursor was spin-cast on ITO substrates at 4000 rpm, and subsequently annealed in ambient at 130°C for 30 min. The ZnO deposited substrates were then transferred into a nitrogen-filled glove box (< 0.1 ppm O<sub>2</sub> and H<sub>2</sub>O).

The binary active layer was prepared by spin-coating a mixture of PTB7-Th: PC<sub>71</sub>BM in chlorobenzene (9 mg/mL for PTB7-Th, 13.5 mg/mL for PC<sub>71</sub>BM) solution with 3% (v/v) 1, 8-diiodooctane (DIO) at 2000 rpm to form a film around 100 nm. For the ternary blend based devices, additional amounts of RTCN with various ratios were added into PTB7-Th: PC<sub>71</sub>BM (1:1.5) solution. After spin-casting, the as-prepared films were put in vacuum for 30 min to remove DIO residue. The PTB7-Th/RTCN binary devices were prepared by spin-casting their chloroform solution (1:1.5, w/w) with 3% (v/v) *N*-methyl-2-pyrrolidone (NMP) as a solvent additive at 5000 rpm for 30 s to form a film with the thickness around 90 nm. Top electrodes were thermally evaporated through a shadow mask onto the active layer. Specifically, the 8.0 nm MoO<sub>3</sub> followed by 80 nm Ag top electrodes were thermally deposited in vacuum at a base pressure of  $3 \times 10^{-6}$  Torr. The active area of the pixels as defined by the overlap of anode and cathode area was 0.096 cm<sup>2</sup>. Four individual devices were simultaneously prepared on each substrate. All the devices were encapsulated in the glove box with the mixture of epoxy and hardener (1:1 in volume) and then covered with a glass slide.

The current density-voltage ( $J$ - $V$ ) characteristics were measured using a Keithley 2400 source measure unit. The photocurrent was measured under AM 1.5G illumination (through the glass substrate) at  $100 \text{ mW/cm}^2$  using a Newport Thermo Oriel 91192 1000W Solar Simulator. Light intensity of the measurement was calibrated with an NREL-certified monocrystalline silicon reference cell. Incident photon conversion efficiency (IPCE) spectra were recorded using the monochromated (Bentham) output from a tungsten halogen lamp calibrated with a Newport UV-181 photodiode; phase sensitive detection with a lock-in amplifier was used to increase signal to noise.

**Other Characterizations.** NMR spectra were recorded on a Bruker Ultra Shield Plus 400 MHz NMR ( $^1\text{H}$ : 400 MHz,  $^{13}\text{C}$ : 100 MHz). The molecular weight of intermediates was measured by a Bruker matrix-assisted laser desorption/ionization time of flight mass spectrometry (MALDI-TOF MS) without using any matrix. UV-Vis spectra were measured with Shimadzu UV-Vis-NIR spectrophotometer. For the photoluminescence, the active layer were pumped with the pulsed (12 ns, 10 Hz) output from a Q-switched Nd:YAG laser pumped optical parametric amplifier (Spectron SL450), focused with a cylindrical lens to form a  $4.10 \text{ mm} \times 0.44 \text{ mm}$  stripe-shaped excitation area on the sample. The emission was monitored with a fiber-coupled spectrograph and a CCD detector from Oriel Instrument. Atom force microscopy (AFM) measurements for surface morphology were conducted on Bruker ScanAsyst AFM in tapping mode. Differential scanning calorimetry (DSC) measurements were performed on Shimadzu DSC-60A equipment. X-ray diffraction (XRD) patterns were recorded by Bruker D8 advance with Cu K $\alpha$  radiation ( $\lambda = 1.5406 \text{ \AA}$ ). The electrochemical behaviors of RTCN were investigated by cyclic voltammetry (CV) with a standard three electrodes electrochemical cell in a 0.1 M tetra-*n*-butylammonium hexafluorophosphate ( $\text{Bu}_4\text{NPF}_6$ ) acetonitrile solution at room temperature under nitrogen with a scanning rate of 100 mV/s. A platinum working electrode, a platinum wire counter electrode

and a reference electrode of Ag/AgNO<sub>3</sub> (0.1 M) were used. The RTCN films for electrochemical measurements were coated from its dilute solution. The energy levels were determined by oxidation and reduction onset. Ferrocene was utilized as the reference. Fluorescence confocal microscopy (FCM) images were measured by a confocal laser scanning microscope system (CLSM, Leica, TCS SP5) with an excitation wavelength of 488 nm. Transmission electron microscopy (TEM) images were recorded on a JEOL 2010 transmission electron microscope at an accelerating voltage of 100 kV. Grazing incidence wide-angle X-ray scattering (GIWAX) analysis was conducted at the BL14B1 beam lines at Shanghai Synchrotron Radiation Facility, China.

The sample preparation procedures for DSC measurements: The prepared PTB7-Th/RTCN chlorobenzene solution with various ratios was stirred overnight, followed by dropped onto a clean glass slide. Then the samples were moved into a vacuum chamber for 12 h to remove the solvents. After being dried, the samples were scratched onto weighting paper and then be ready for DSC measurements.

## **Materials**

All reagents and solvents for synthesis, unless otherwise specified, were obtained from Aldrich and TCI Chemical Co and used as received. All manipulations involving air sensitive reagents were performed under an atmosphere of dry argon. PTB7-Th and PC<sub>71</sub>BM were purchased from Lumtec co. and Solenne, respectively. Zinc acetate dehydrate (Zn(CH<sub>3</sub>COO)<sub>2</sub>·2H<sub>2</sub>O, 99.95%) was purchased from Aldrich. All the materials for polymer solar cells fabrication were used as received.

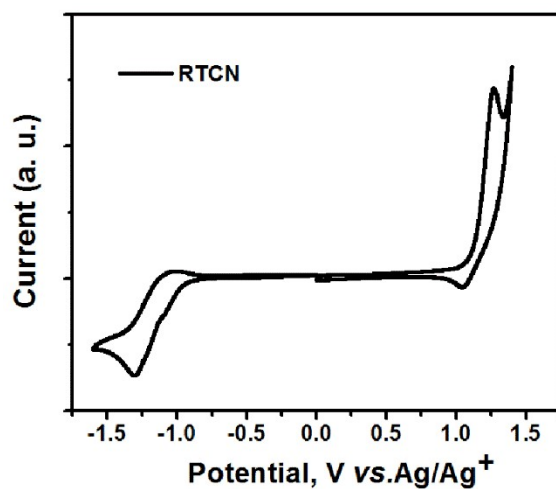


**Figure S1.** Oxidative and reductive cyclic voltammetry plots of RTCN measured in film states.

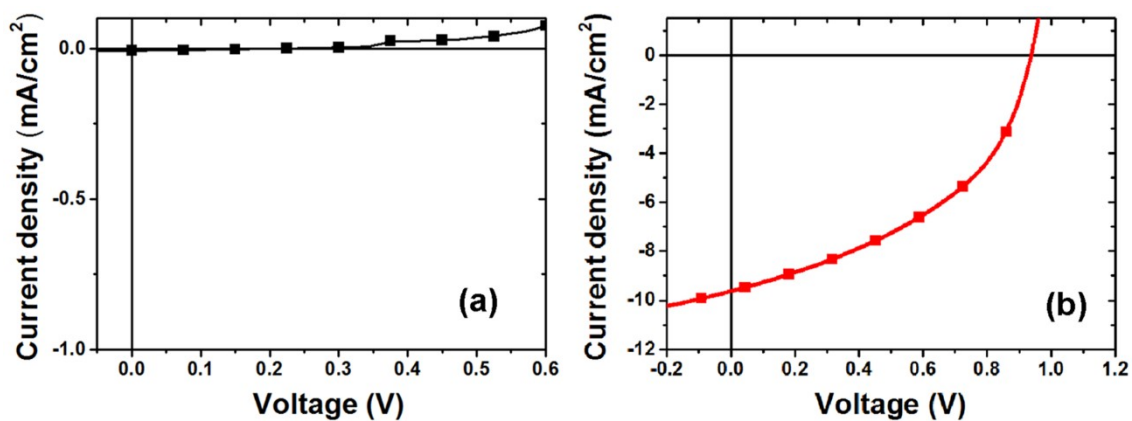


**Figure S2.**  $J$ - $V$  characteristics under AM 1.5G irradiation at 100 mW/cm<sup>2</sup> of the (a) RTCN: PC<sub>71</sub>BM (1:1) binary device; (b) optimized PTB7-Th: RTCN (1:1.5) binary device. The device architecture was ITO/ZnO/active layer/MoO<sub>3</sub>/Ag.

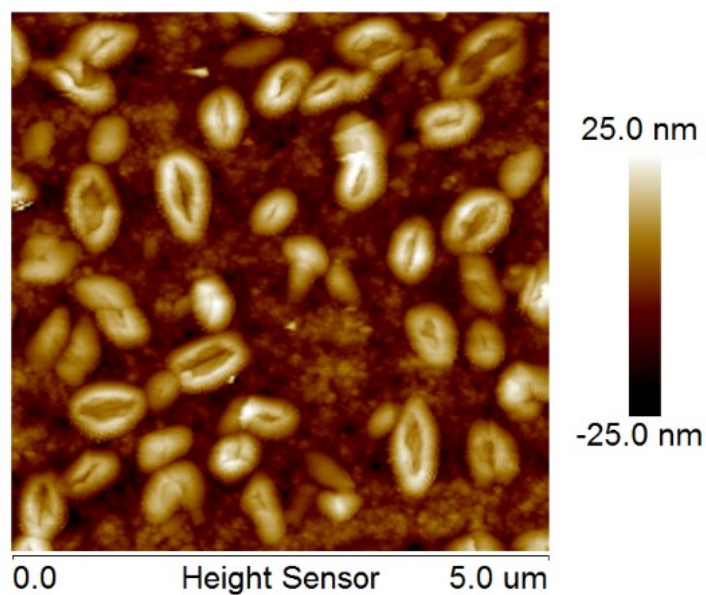


**Figure S3.** Atomic force microscopy (AFM) images of PTB7-Th: RTCN (1:1.5) binary blend films coated from their chloroform/*N*-methyl-2-pyrrolidone (97:3, v/v) solution.

The binary PTB7-th: RTCN films show micrometer-scaled crystalline domains. Similar morphologies and the influence on crystalline domains size have been well-studied from previous studies on *N*, *N*'-bis(1-ethylpropyl)-perylene-3,4,9,10-tetracarboxylic diimide (EP-PDI) based solar cells.<sup>[2]</sup>

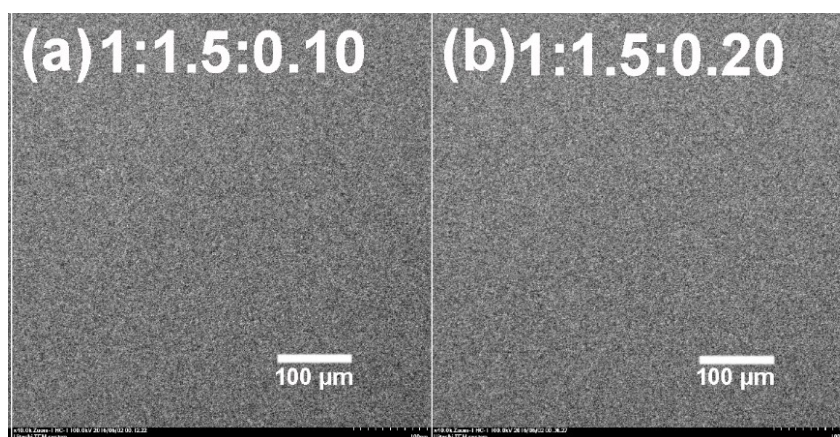


**Figure S4.** TEM images for the films of ITO/ZnO/ PTB7-Th: PC<sub>71</sub>BM: RTCN with various ratios. The all bars were set at 100 μm.

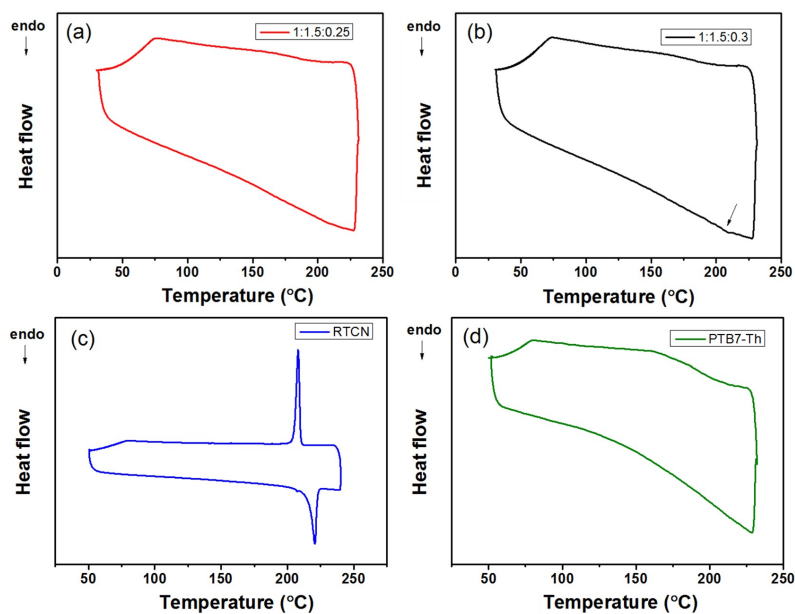


**Figure S5.** DSC traces of the materials with various components: (a) PTB7-Th:PC<sub>71</sub>BM:RTCN = 1:1.5:0.25, (b) PTB7-Th:PC<sub>71</sub>BM:RTCN = 1:1.5:0.30, (c) pure RTCN, (d) pure PTB7-Th. All these data were recorded at a heating rate of 10°C min<sup>-1</sup>.

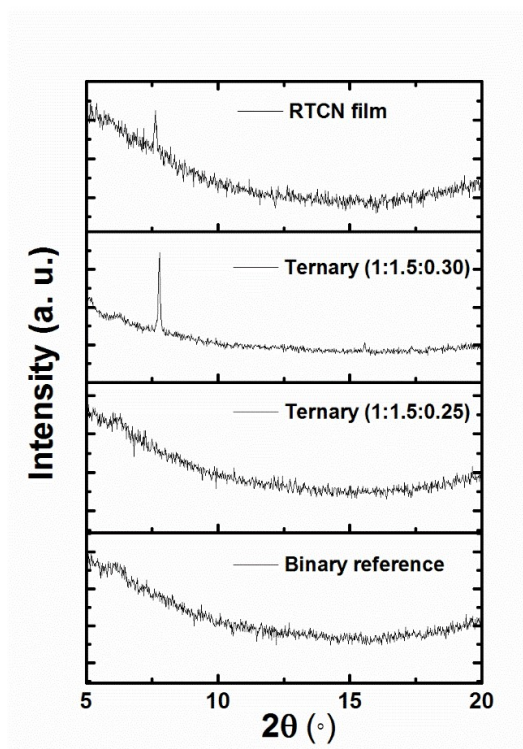


**Figure S6.** XRD patterns for the films prepared by the solution of PTB7-Th: PC<sub>71</sub>BM (1: 1.5), PTB7-Th: PC<sub>71</sub>BM: RTCN with ratios of 1: 1.5: 0.25 and 1: 1.5: 0.30, and pure RTCN. For all the cases, the used solution was chlorobenzene.



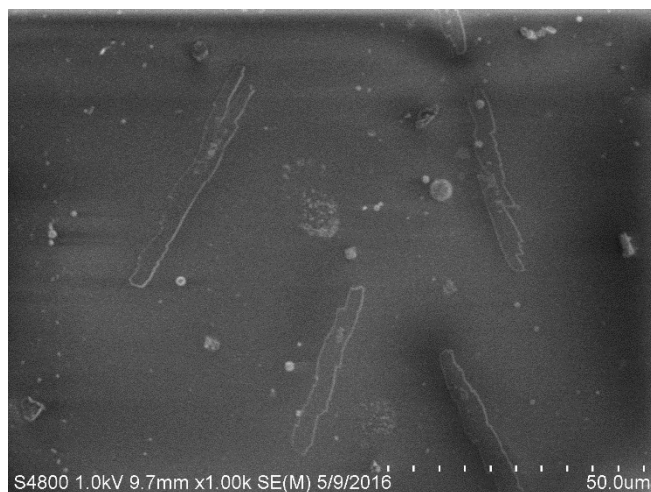


**Figure S7.** SEM images for the film of ITO/ZnO/ PTB7-Th: PC<sub>71</sub>BM: RTCN (1:1.5:0.30). The all bars were set at 50 μm.

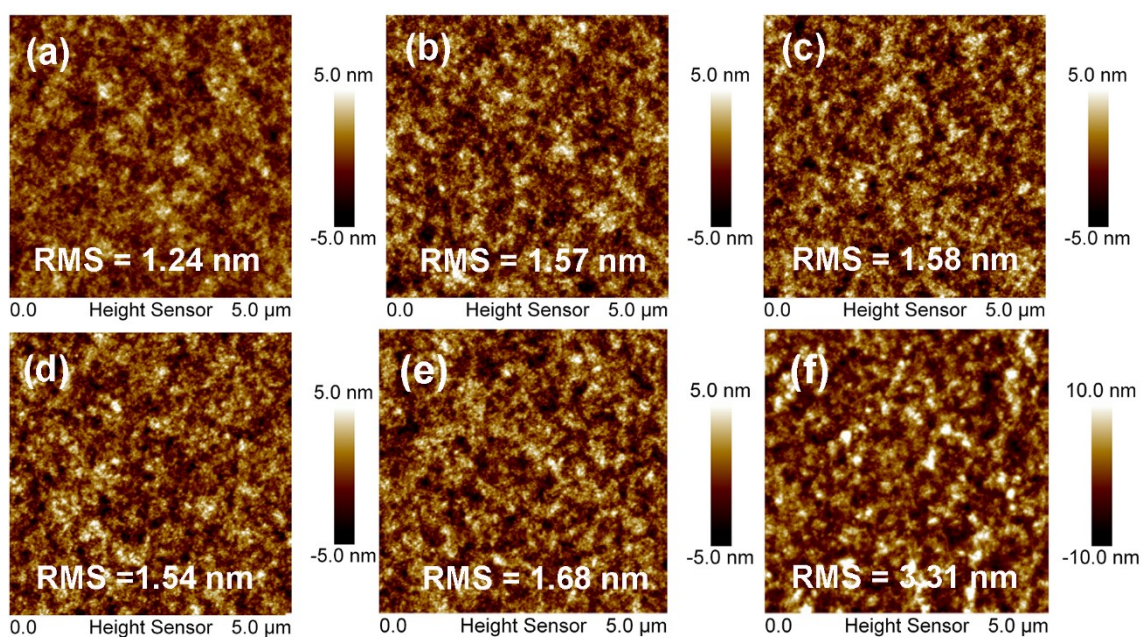


**Figure S8.** Atomic force microscopy (AFM) images of (a) PTB7-Th:PC<sub>71</sub>BM = 1:1.5; (b) PTB7-Th:PC<sub>71</sub>BM:RTCN = 1:1.5:0.10; (c) PTB7-Th:PC<sub>71</sub>BM:RTCN = 1:1.5:0.20; (d) PTB7-Th:PC<sub>71</sub>BM:RTCN = 1:1.5:0.25; (e) PTB7-Th:PC<sub>71</sub>BM:RTCN = 1:1.5:0.30; (f) PTB7-Th:PC<sub>71</sub>BM: RTCN = 1:1.5:0.40 on top of ITO/ZnO substrates.



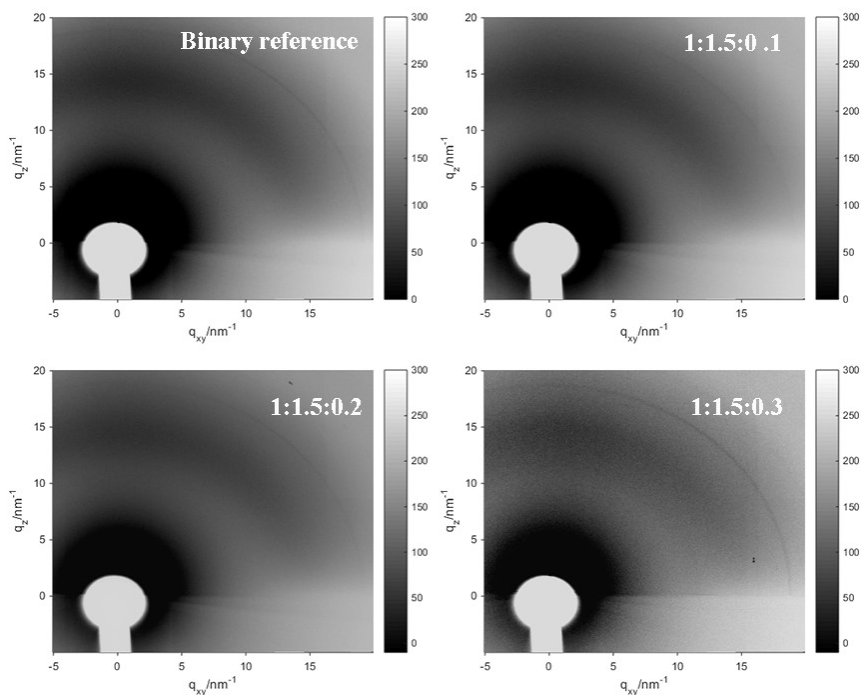


**Figure S9.** 2D GIWAXS patterns with different ratios of PTB7-Th:PC<sub>71</sub>BM:RTCN.

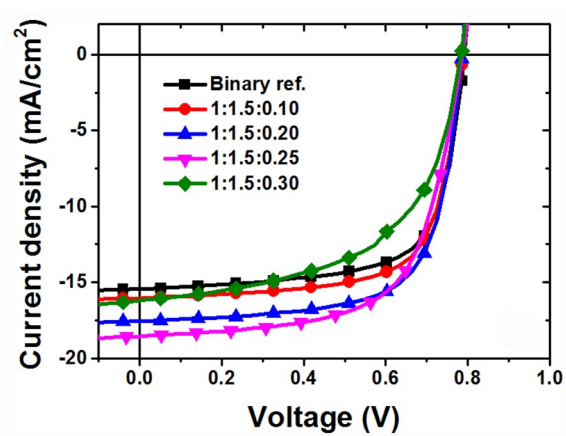


**Figure S10.**  $J$ - $V$  characteristics under AM 1.5G irradiation at  $100 \text{ mW/cm}^2$  of the best binary reference and the ternary blend devices with the highest efficiency. The device architecture was ITO/ZnO/active layer/MoO<sub>3</sub>/Ag.

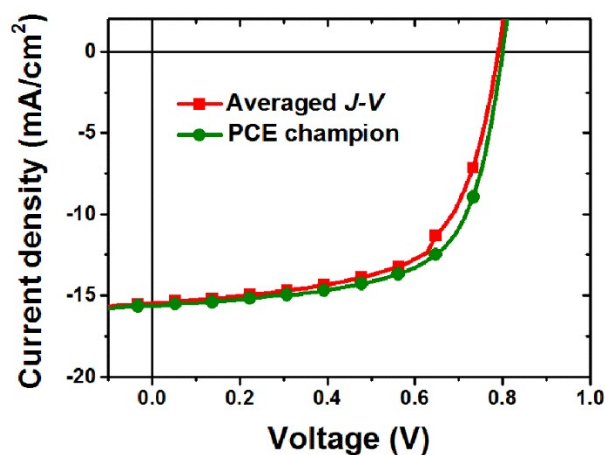


**Figure S11.** The averaged  $J$ - $V$  characteristics and the best performance of the binary PTB7-Th: PC<sub>71</sub>BM (1:1.7, w/w) devices under AM 1.5G irradiation at 100 mW/cm<sup>2</sup>. The device architecture was ITO/ZnO/PTB7-Th: PC<sub>71</sub>BM /MoO<sub>3</sub>/Ag.

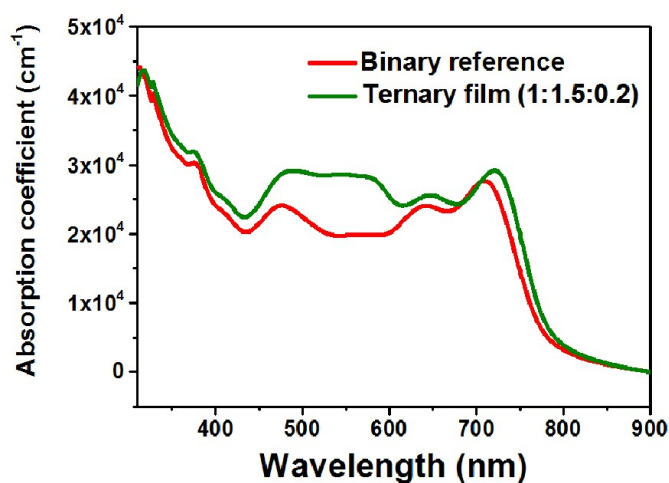


**Figure S12.** Absorption coefficient spectra of the reference binary film and the ternary blend films with optimized RTCN loading (1:1.5:0.20). The film thickness is 92 nm for the PTB7-Th/PC<sub>71</sub>BM binary blend film and 109 nm for the PTB7-Th/PC<sub>71</sub>BM/CRTCN (1:1.5:0.2) film, respectively.

**Table S1.** Photovoltaic performances of the polymer solar cells with binary acceptor systems in literature.

Binary Host	The second acceptor	Device configuration	PCE champion (Binary) (%)	PCE champion (Ternary) (%)	ref
P3HT/OXCMA (IC <sub>60</sub> MA)	OXCTA (IC <sub>60</sub> BA)	conventional	3.61	3.96	3
PTBT/PC <sub>71</sub> BM	PC <sub>61</sub> BM	conventional	5.91	7.00	4
PTB7/PC <sub>71</sub> BM	IC <sub>60</sub> BA	conventional	7.23	8.13	5
PTB7/PC <sub>71</sub> BM	IC <sub>60</sub> BA	inverted	7.52	7.18	6
DR3TBDTT/IC <sub>60</sub> BA	PC <sub>71</sub> BM	conventional	3.45	5.11	7
PTB7-Th/PC <sub>71</sub> BM	RTCN	inverted	8.50	9.55	This work

The dependence of  $J_{SC}$  upon light intensity is according to the following equation:

$$J_{sc} \propto I^\alpha$$

The equation for light intensity dependent  $V_{OC}$  is:

$$V_{oc} = \frac{E_{gap}}{q} - \frac{kT}{q} \ln \left[ \frac{(1 - P_D)\gamma N_c^2}{P_D G} \right]$$

where  $E_{gap}$  is the energy level difference between the highest occupied molecular orbital (HOMO) of the donor material and lowest unoccupied molecular orbital (LUMO) of the acceptor,  $q$  is the elementary charge,  $k$  is the Boltzmann constant,  $T$  is temperature in Kelvin,  $P_D$  is the dissociation probability of the electron-hole pairs,  $\gamma$  is the Langevin recombination constant,  $N_C$  is the effective density of states, and  $G$  is the generation rate of bound electron-hole pairs.

The mobility was measured in the hole-only devices with the structure of ITO/PEDOT:PSS/active layer/MoO<sub>3</sub>/Au, and the electron mobility was measured in the electron-only devices with structure of ITO/ZnO/active layer/LiF/Al, and determined in the space charge limited current (SCLC) regime by Mott-Gurney law. The used fitting equation is described as following:

$$J = \frac{9}{8} \varepsilon_0 \varepsilon_r \mu_0 e^{0.833\gamma\sqrt{E}} \frac{V^2}{L^3}$$

Where  $\varepsilon_0$  is the permittivity of free space,  $\varepsilon_r$  is the dielectric constant of the polymer,  $V$  is the voltage drop across the device, and  $L$  is the active layer thickness,  $E$  is the electric field,  $\mu_0$  the zero-field mobility, and  $\gamma$  the field dependence prefactor. The value of  $\varepsilon_r$  is assumed to be 3, which is a typical value for a conjugated polymer.

The utilized work function values of the electrodes are -5.2 eV to ITO/PEDOT:PSS, -5.1 eV for Au, -4.4 eV for ITO/ZnO and -2.9 eV for LiF/Al.<sup>[8-10]</sup>

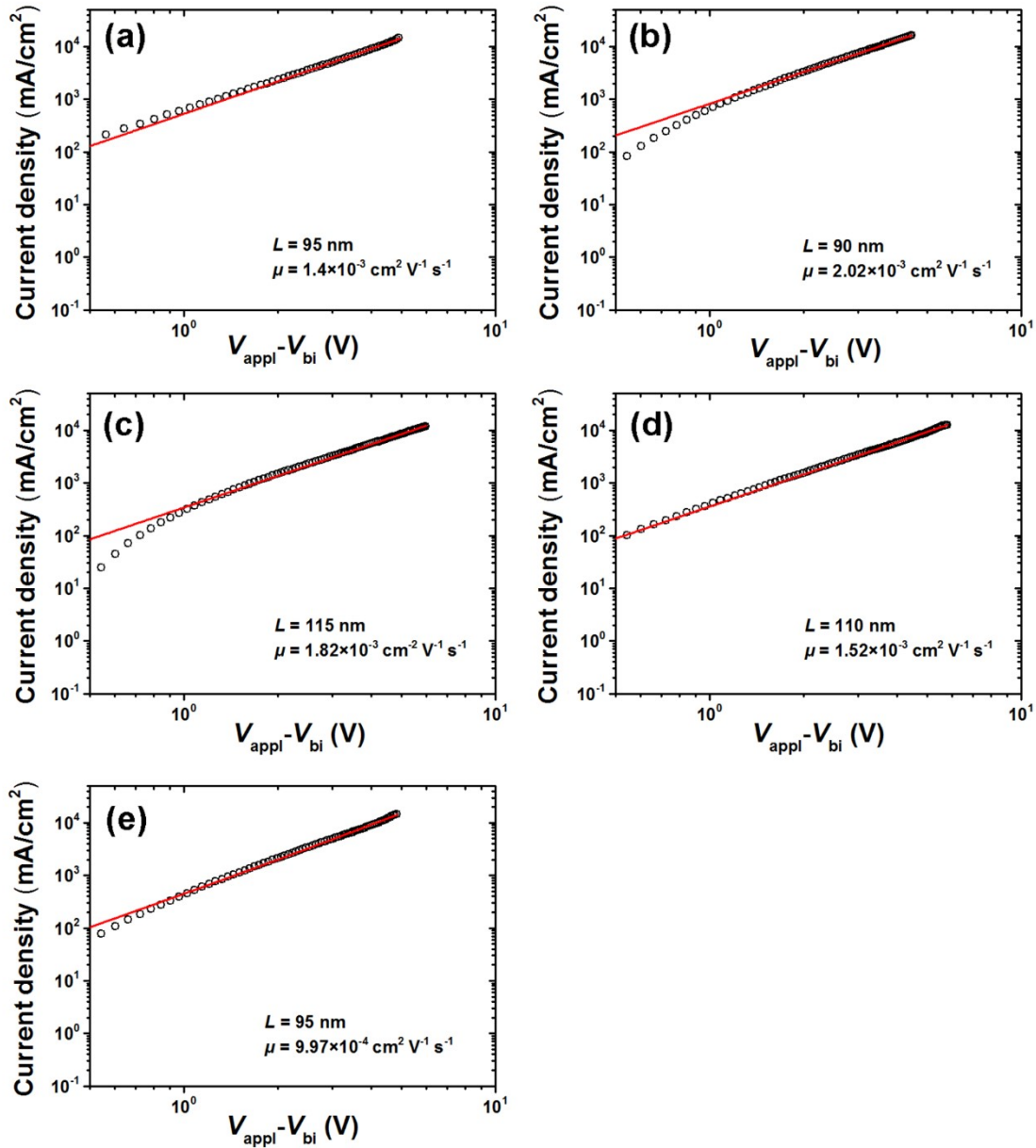


**Figure S13.** Representative  $J$ - $V$  curves for the hole-only diodes for estimation of hole mobilities using an SCLC model. (a) PTB7-Th: PC<sub>71</sub>BM = 1:1.5; (b) PTB7-Th:PC<sub>71</sub>BM:RTCN = 1:1.5:0.10; (c) PTB7-Th:PC<sub>71</sub>BM:RTCN = 1:1.5:0.20; (d) PTB7-Th:PC<sub>71</sub>BM:RTCN = 1:1.5:0.25; (e) PTB7-Th:PC<sub>71</sub>BM:RTCN = 1:1.5:0.30.



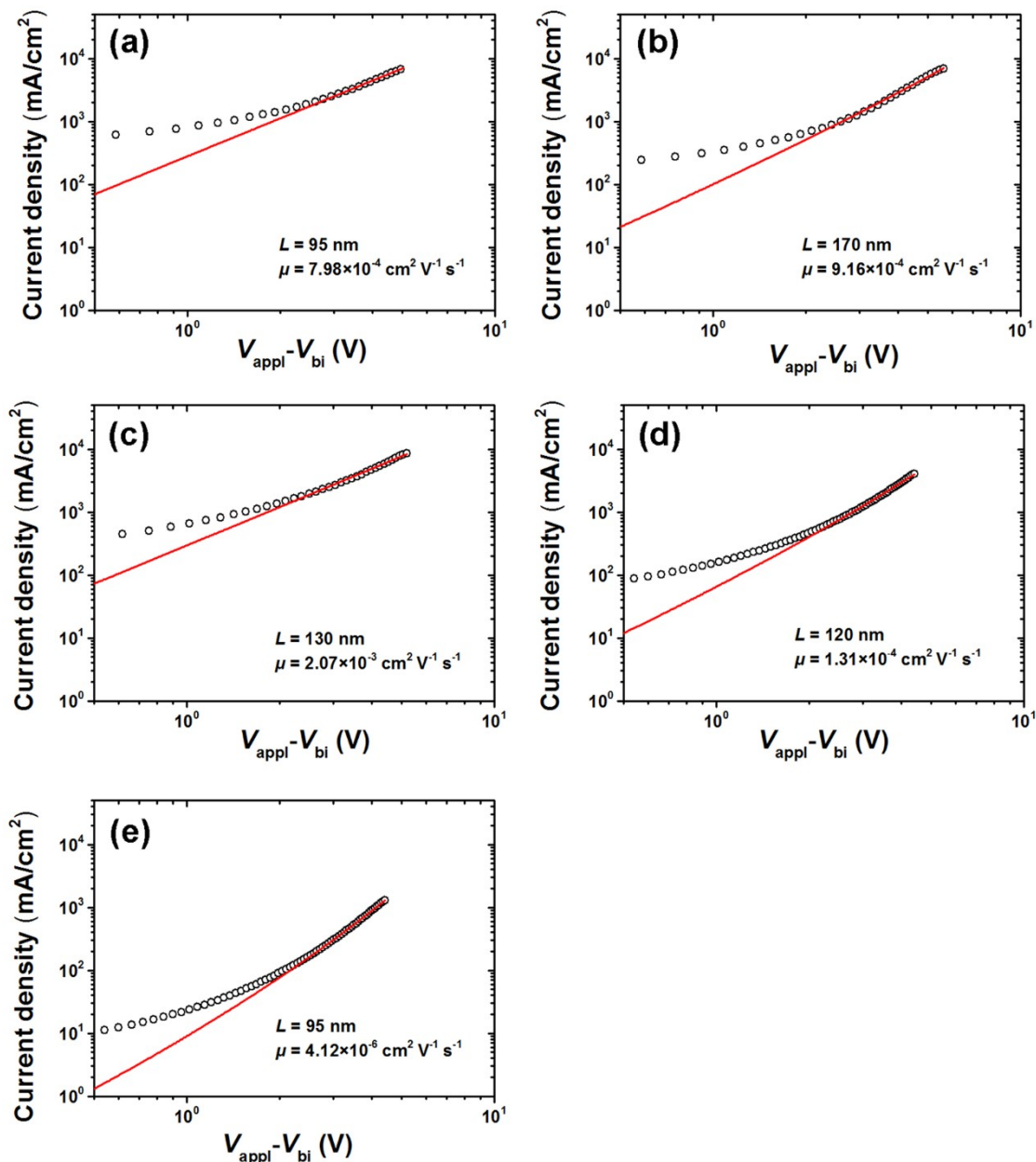
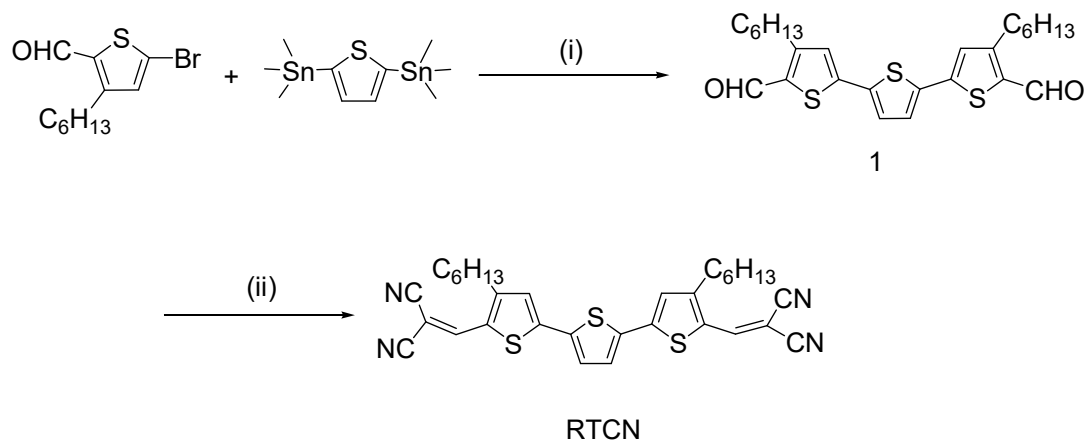


**Figure S14.** Representative  $J$ - $V$  curves for the electron-only diodes for estimation of electron mobilities using an SCLC model. (a) PTB7-Th:PC<sub>71</sub>BM = 1:1.50; (b) PTB7-Th:PC<sub>71</sub>BM:RTCN = 1:1.50:0.10; (c) PTB7-Th:PC<sub>71</sub>BM:RTCN = 1:1.50:0.20; (d) PTB7-Th:PC<sub>71</sub>BM:RTCN = 1:1.50:0.25; (e) PTB7-Th:PC<sub>71</sub>BM:RTCN = 1:1.50:0.30.

## Synthesis and Characterization



**Scheme S1** (i) Pd(PPh<sub>3</sub>)<sub>4</sub>, toluene, 110 °C; (ii) triethylamine, malononitrile, chloroform, rt..

### 5-(5-(5-formyl-4-hexylthiophen-2-yl)thiophen-2-yl)-3-hexylthiophene-2-carbaldehyde

**(1):** 5-bromo-3-hexylthiophene-2-carbaldehyde (200 mg, 0.73 mmol), 2,5-bis(trimethylstannyl)thiophene (654 mg, 1.6 mmol), Pd(PPh<sub>3</sub>)<sub>4</sub> (25 mg, 0.02 mmol) were dissolved in toluene (10 mL) in a degassed vessel. The mixture was heated at 110 °C for 24 h. After cooling down, the mixture was diluted with chloroform and washed by brine for three times. The organic phase was combined and dried over MgSO<sub>4</sub>. After the solvent was removed, the residue was purified by silica gel column using hexane/dichloromethane (1:1) as the eluent to give **1** as a dark yellow solid (320 mg, 93.2%). <sup>1</sup>H NMR (400 MHz, CDCl<sub>3</sub>): δ 9.94 (s, 2H), 7.18 (s, 2H), 7.03 (s, 2H), 3.01 – 2.81 (m, 4H), 1.70 – 1.60 (m, 4H), 1.39 – 1.25 (m, 12H), 0.86 (t, *J* = 7.0 Hz, 6H). <sup>13</sup>C NMR (100 MHz, CDCl<sub>3</sub>): δ 182.41, 146.98, 146.98, 144.44, 141.51, 139.67, 137.39, 135.99, 134.18, 126.89, 125.87, 124.32, 123.93, 120.13, 31.66, 30.48, 30.36, 28.97, 22.61, 14.10. MALDI-TOF-MS (*m/z*): Calcd for C<sub>26</sub>H<sub>32</sub>O<sub>2</sub>S<sub>3</sub>, Exact Mass: M<sup>+</sup> 472.16; Found: 471.83 (M<sup>+</sup>).

**RTCN:** Malononitrile (69.9 mg, 1.1 mmol) and **1** (200 mg, 0.42 mmol) were dissolved in 20 ml of CHCl<sub>3</sub>, and then 0.1 mL of triethylamine was added. The solution was stirred at room temperature for 1 h. The mixture was then diluted with chloroform and washed by brine for three times. The organic phase was combined and dried over MgSO<sub>4</sub>. After the solvent was removed, the resulting residue was purified by column

chromatography using hexane as the eluent to give **RTCN** as a dark red solid (210 mg, 90.5%).  $^1\text{H}$  NMR (400 MHz,  $\text{CDCl}_3$ ):  $\delta$  7.84 (s, 2H), 7.40-7.39 (d, 2H), 7.14 (s, 1H), 2.77-2.73 (t, 4H), 1.66-1.63 (m, 4H), 1.36-1.31 (m, 12H), 0.93-0.89 (t, 6H).  $^{13}\text{C}$  NMR (100 MHz,  $\text{CDCl}_3$ ):  $\delta$  157.08, 147.56, 145.77, 137.41, 129.61, 128.30, 126.71, 114.73, 113.63, 31.50, 31.21, 29.26, 29.03, 22.52, 14.05. MALDI-TOF-MS ( $m/z$ ): Calcd for  $\text{C}_{32}\text{H}_{32}\text{N}_4\text{S}_3$ , Exact Mass:  $M^+$  568.18; Found: 567.97 ( $M^+$ ).

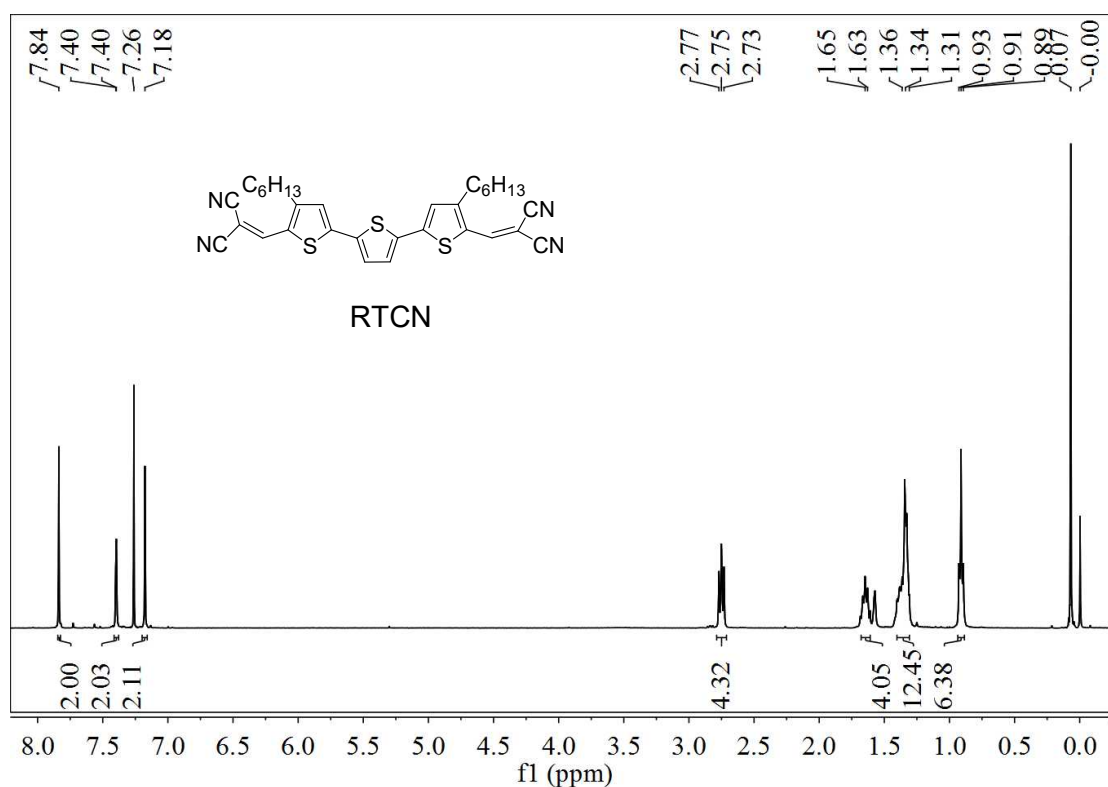


**Figure S15.**  $^1\text{H}$  NMR spectra for RTCN.

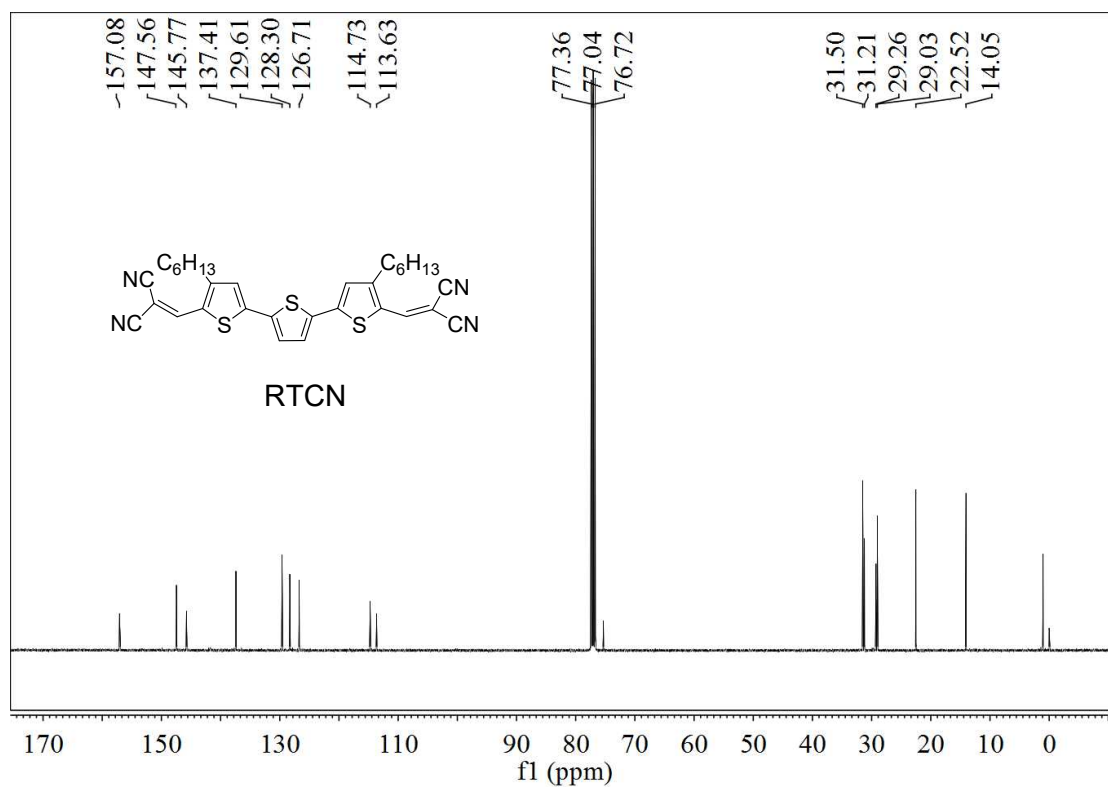


Figure S16.  $^{13}\text{C}$  NMR spectra for RTCN.

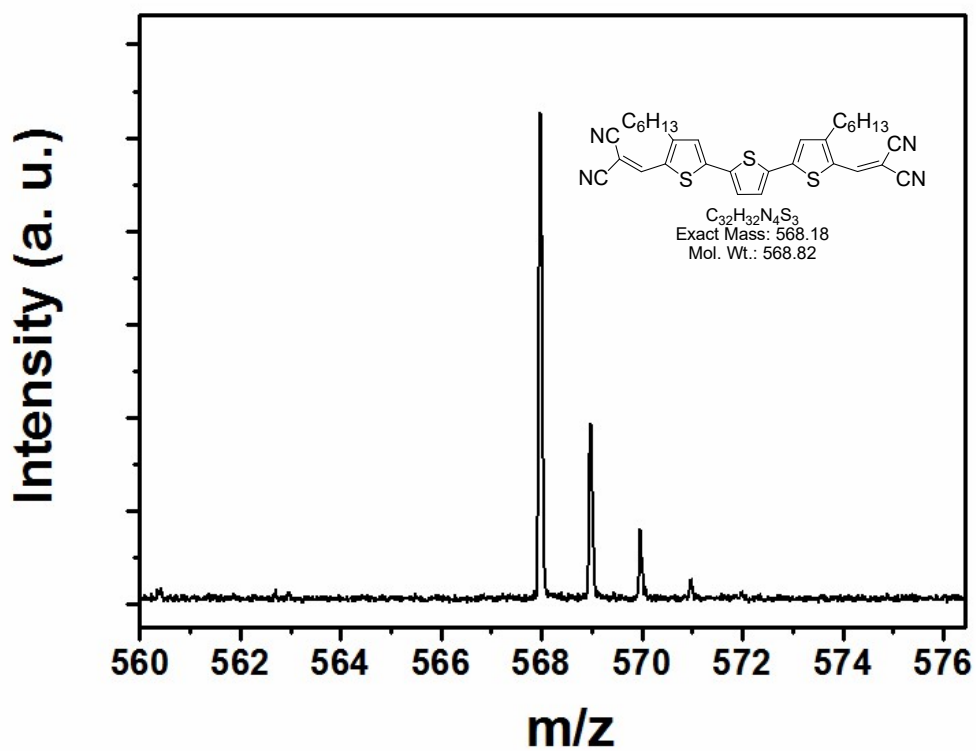


Figure S17. MALDI-TOF-MS spectra for RTCN.

## References:

- [1] Y. Sun, J. H. Seo, C. J. Takacs, J. Seiffter, A. J. Heeger, *Adv. Mater.* **2011**, *23*, 1679.
- [2] T. Ye, R. Singh, H. Butt, G. Floudas, P. E. Keivanidis. *ACS Appl. Mater. Interfaces* **2013**, *5*, 11844.
- [3] H. Kang, K.-H. Kim, T. E. Kang, C.-H. Cho, S. Park, S. C. Yoon, B. J. Kim, *ACS Appl. Mater. Interfaces* **2013**, *5*, 4401.
- [4] S.-J. Ko, W. Lee, H. Choi, B. Walker, S. Yum, S. Kim, T. J. Shin, H. Y. Woo, J. Y. Kim, *Adv. Energy Mater.* **2014**, 1401687.
- [5] P. Cheng, Y. F. Li, X. Zhan, *Energy Environ. Sci.* **2014**, *7*, 2005.
- [6] R. Sharma, H. Lee, V. Gupta, H. Kim, M. Kumar, C. Sharma, S. Chand, S. Yoo, D. Gupta, *Org. Electron.* **2016**, *34*, 111.
- [7] Y. J. Kim, J. Hong, C. E. Park, *ACS Appl. Mater. Interfaces* **2015**, *7*, 21423.
- [8] T. M. Brown, J. S. Kim, R. H. Friend, F. Cacialli, R. Daik, W. J. Feast, *Appl. Phys. Lett.* **1999**, *75*, 1679.
- [9] W. Xu, Z. Kan, T. L. Ye, L. Zhao, W.-Y. Lai, R. Xia, G. Lanzani, P. E. Keivanidis, W. Huang, *ACS Appl. Mater. Interfaces* **2015**, *7*, 452.
- [10] L.-M. Chen, Z. Xu, Z. Hong, Y. Yang, *J. Mater. Chem.* **2010**, *20*, 2575.